Space Launch System acoustics: Far-field noise measurements of the Artemis-I launch

Cite as: JASA Express Lett. **3**, 023601 (2023); https://doi.org/10.1121/10.0016878
Submitted: 29 November 2022 • Accepted: 30 December 2022 • Published Online: 14 February 2023

Kent L. Gee, Grant W. Hart, Carson F. Cunningham, et al.

JASA EXPRESS LETTERS ARTICLE asa.scitation.org/journal/jel

Space Launch System acoustics: Far-field noise measurements of the Artemis-I launch

Kent L. Gee,[1,a)] Grant W. Hart,[1] Carson F. Cunningham,[1] Mark C. Anderson,[1]
Michael S. Bassett,[1] Logan T. Mathews,[1] J. Taggart Durrant,[1] Levi T. Moats,[1] Whitney L. Coyle,[2]
Makayle S. Kellison,[2] and Margaret J. Kuffskie[2]
[1]*Department of Physics and Astronomy, Brigham Young University, Provo, Utah 84602, USA*
[2]*Department of Physics, Rollins College, Winter Park, Florida 32789, USA*
kentgee@byu.edu, grant_hart@byu.edu, carsonfc@byu.edu, mark.c.anderson@byu.edu, mibuscus@byu.edu, lmathew3@byu.edu, jdurran4@byu.edu, lmoats@byu.edu, wcoyle@rollins.edu, mkellison@rollins.edu, mkuffskie@rollins.edu

Abstract: To improve understanding of super heavy-lift rocket acoustics, this letter documents initial findings from noise measurements during liftoff of the Space Launch System's Artemis-I mission. Overall sound pressure levels, waveform characteristics, and spectra are described at distances ranging from 1.5 to 5.2 km. Significant results include: (a) the solid rocket boosters' ignition overpressure is particularly intense in the direction of the pad flame trench exit; (b) post-liftoff maximum overall levels range from 127 to 136 dB, greater than pre-launch predictions; and (c) the average maximum one-third-octave spectral peak occurred at 20 Hz, causing significant deviation between flat and A-weighted levels.

[Editor: Tracianne B. Neilsen] https://doi.org/10.1121/10.0016878

Received: 29 November 2022 **Accepted:** 30 December 2022 **Published Online:** 14 February 2023

1. Introduction

On 16 November 2022, at 1:47 am Eastern Standard Time, NASA's Space Launch System (SLS) lifted off from Kennedy Space Center (KSC), to become the world's most powerful rocket successfully launched. The Artemis-I version of SLS, with a liftoff thrust of 39.1 MN (8.8×10^6 lb), exceeded the thrust of the previous record holder, the Saturn V, by about 13%.

This letter's purpose is to briefly report on sound levels and other noise characteristics measured at different locations around KSC using state-of-the-art acoustical instrumentation. Acoustical measurements of SLS extend our ability to understand launch vehicle noise beyond prior measurements. As more powerful super heavy-lift vehicles, i.e., SpaceX's Starship/Super Heavy and SLS Block 2, are being developed, these data can be used for validation of existing noise prediction models (Eldred, 1971; McInerny, 1992; Margasahayam and Caimi, 1999; James *et al.*, 2020b) and creation of improved ones. Accurate noise models are needed to quantify and mitigate possible damage to launch pads, vehicles, and payloads as well as quantify community and environmental impacts. Although more in-depth studies will eventually be published, we hope these timely results prevent the propagation of SLS acoustics misinformation, like the apocrypha that surrounded the Saturn V for over 50 years (Gee *et al.*, 2022). We anticipate this letter will act as a reliable initial resource for acousticians, rocket scientists, and the general public.

2. Vehicle and launch description

The successful nighttime launch of SLS was both visually and acoustically impressive. Figure 1 shows NASA and United Launch Alliance photos of SLS during Artemis-I liftoff. While Fig. 1(a) shows the scale of the 98.1 m tall rocket relative to Launch Complex 39B (LC-39B), Fig. 1(b) clearly shows the core stage being powered by four Aerojet Rocketdyne RS-25 liquid hydrogen-oxygen engines with about 7200 kN total maximum thrust. On opposite sides of the core stage are two Northrop Grumman five-segment solid-fuel rocket boosters (SRBs) that each provided around 16 000 kN thrust. Given their relative contribution to total SLS thrust, the SRBs likely dominate the overall noise radiation, as they did during Space Shuttle launches (McInerny, 1992).

The Artemis-I launch timing provided a unique opportunity to visualize propagating pressure waves during liftoff. A recent article about the Saturn-V noise (Gee *et al.*, 2022) noise included a video of the Apollo-17 liftoff, during which sound waves were made visible because of the nighttime launch window, humidity, and backlighting. High-intensity pressure rarefactions caused the local atmospheric pressure to fall below the vapor pressure and condensation to occur,

[a)]Author to whom correspondence should be addressed.

Fig. 1. Liftoff of the Artemis I mission from Kennedy Space Center. (a) Wide-angle view of LC-39B as viewed from the southwest. Photo credit: NASA. (b) The two SRBs and four RS-25 engines. Photo credit: United Launch Alliance. Used with permission.

such that a rarefaction was visible as a rapidly propagating cloud that disappeared as the intensity decayed with distance. We recognized a similar opportunity here and a compilation of NASA Artemis-I liftoff videos from different angles in Mm. 1 contains visible rarefactions at liftoff. Of particular mention is the propagating pressure wave from the SRB ignition overpressure (IOP) that appears at $t = 0$ s and, in the bottom-left video, propagates to the right of the mobile launcher in the direction of the flame trench exit. This rarefaction cloud is rapidly followed by other visible rarefactions, likely due to high-intensity Mach waves radiated from the supersonic, flame trench-deflected exhaust plumes (Lubert *et al.*, 2022).

Mm. 1. Time-synchronized compilation of four NASA videos showing visible pressure rarefactions during SLS liftoff. This is a file of type ".mp4" (25 MB). Original footage online (NASA, 2022).

3. Measurement description

Acoustic data were collected at several far-field sites surrounding LC-39B, both inside and outside KSC, but all beyond the limit imposed by the 1350-m radius blast danger area. In an attempt to strike a balance between completeness, conciseness, and clarity, the data analyzed here are limited to a subset of five stations located between 1.4 and 5.2 km from the pad. Shown in Fig. 2(a) are station numbers and distances from the center of LC-39B as well as some other points of interest. The remaining stations will be analyzed in detail and discussed in future publications.

Data were collected using an in-house system referred to as the Portable Unit for Measuring Acoustics (PUMA), which consisted of a ruggedized computer, a GPS time clock for synchronization, NI 9250 24-bit/5-V data acquisition modules sampling at 102.4 kHz, and a lithium-ion battery housed in a weatherproof case, along with a solar charging system (Gee *et al.*, 2020). Microphones used with the PUMAs were condenser, free-field microphones: 6.35 mm (1/4 in.) diameter GRAS 46BE (4 Hz–80 kHz), except at Station 4, which used the 12.7 mm (1/2 in.) 47AC microphone (0.09 Hz–20 kHz). The 47AC was used to obtain the true low-frequency spectral slope in the event any roll-off of the 46BEs' responses was observable below 4 Hz.

The microphone configuration used at each PUMA was a weather-robust custom ground plate design developed for rocket launches (James *et al.*, 2020a) and further developed for sonic boom measurements (Gee *et al.*, 2020; Anderson *et al.*, 2022). This configuration consists of a microphone inverted above a plastic circular ground plate under a thick porous polyurethane foam windscreen. Figure 2(b) shows the setup arranged in a triangular 2D intensity probe configuration at Station 7, along the LC-39B "Crawlerway." Figure 2(c) shows a closeup of a ground plate setup at Station 3, with SLS slightly visible in the distance. These autonomous PUMA and ground-plate setups have been used in multiple measurements over several years, including prior rocket launches [e.g., James *et al.* (2020a), Hart *et al.* (2022), and Mathews *et al.* (2021)] and sonic booms (Gee *et al.*, 2020).

4. Analysis

As this letter's purpose is to provide early results about the Artemis-I launch noise, findings are limited to overall sound pressure level (OASPL) and some waveform and spectral characteristics. First, Fig. 2 includes the maximum 1 s-averaged OASPL during liftoff for each measurement site. At Station 7, the maximum level after vehicle liftoff was about 136 dB (re 20 μPa, the standard reference pressure in air). At Station 4, near the Saturn-V viewing area, the maximum OASPL was approximately 128 dB. Figure 2 shows that Station 2's maximum OASPL was 1.6 dB lower than that at Station 4, despite being nearly 1 km closer to the pad.

We note that all these maximum levels are much greater than those predicted in an environmental assessment for proposed multi-use of LC-39 (NASA, 2013) and later adopted as part of a "Finding of No Significant Impact" document by the Federal Aviation Administration (2016). Based on prior modeling (NASA, 2008) of the Ares-V rocket with nearly

Fig. 2. (a) Google Earth image annotated to show the measurement stations analyzed in this letter and their distances from LC-39B, as well as other locations of interest: SLS (not to scale) at LC-39B, the Vehicle Assembly Building (VAB), Saturn-V viewing area, and the Crawlerway between the VAB and LC-39B. Shown also are the maximum 1-s OASPLs at each station after liftoff. (b) A four-microphone array at Station 7, in the middle of the Crawlerway. (c) A closeup of a weather-robust microphone ground plate setup at Station 3, with SLS in the background.

40% greater thrust than Artemis-I SLS, the assessment indicated that the OASPL would drop below 110 dB at 4.5 km. A nearly 20 dB measured deviation from that prediction at comparable distances during the Artemis-1 launch suggests a need to revise those models.

Recorded waveforms at Station 7 (1.48 km to the south of LC-39B) and Station 9 (1.78 km to the north) illustrate different aspects of SLS noise radiation around liftoff. Figures 3(a) and 3(b) show the recorded pressure waveforms at Stations 7 and 9, respectively, with the corresponding 1-s-averaged running OASPL shown in Figs. 3(c) and 3(d). Colored markers are located in both sets of plots to illustrate three events that are shown (with corresponding colors) for both stations in subsequent figure panels: RS-25 startup in Figs. 3(e) and 3(f), SRB IOP in Figs. 3(g) and 3(h), and a 0.5 s interval in Figs. 3(i) and 3(j) within the maximum 1-s OASPL window. This maximum level is typically associated with the plume peak noise emission angle, which is controlled by Mach wave radiation from the supersonic exhaust plume (McInerny, 1992). For Shuttle SRBs and an observer on the ground, this maximum noise radiation occurred when the launch vehicle was around 25° above the horizon (Lubert *et al.*, 2022).

For both stations, the RS-25 startup (at around $t = -4.5$ s) is clearly visible, followed by SRB ignition. Given that the LC-39B flame trench exits toward the north, both the RS-25 startup and SRB IOP amplitudes are much greater at Station 9 [Figs. 3(f) and 3(h)] than Station 7 [Figs. 3(e) and 3(g)]. This quantitatively confirms what was seen in Mm. 1: pressure waves of greater intensity in the direction of the flame trench exit. It also shows the importance of detailed measurements and modeling around the pad, as a nearly 400 Pa IOP rarefaction at Station 9 translates to a peak level of 146 dB. Assuming spherical spreading holds (and it may not), the IOP rarefaction would reach 40 kPa (186 dB peak level) at 18 m, a significant fraction of atmospheric pressure. Because of its potential for damaging pad structures and vehicles, IOP measurement, modeling, and mitigation have been the subject of numerous studies [e.g., Ikawa and Laspesa (1985) and Nance and Liever (2015)].

The asymmetry in RS-25 ignition and SRB IOP radiation at Stations 7 and 9 is caused by launch pad geometry and deflected plume direction. Turning to the maximum OASPL post-liftoff at these two stations, their level difference from Fig. 2(a) is 1.9 dB, with Station 7 now having the greater level. This can be explained by the station distances. Assuming far-field spherical spreading, the distance ratio translates into an additional 1.6 dB expected reduction in level at Station 9 relative to Station 7. The agreement between the measured and predicted differences suggests that, although the

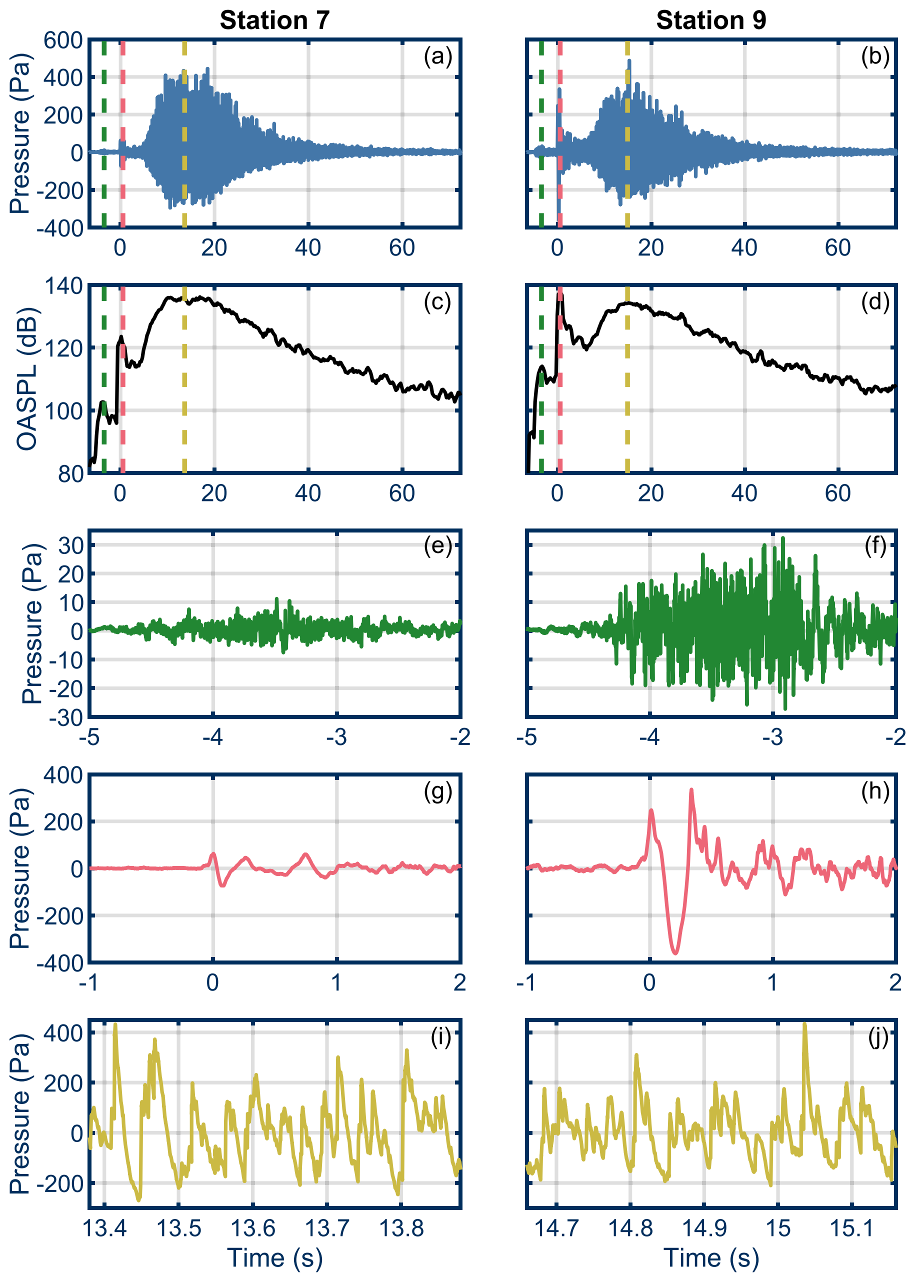

Fig. 3. Waveforms segments at Stations 7 and 9 during the Artemis 1 launch. Left panels are for Station 7, right panels are for Station 9: (a) and (b) Annotated waveform, showing RS-25 startup, SRB ignition, and maximum 1-s OASPL; (c) and (d) Annotated 1-s running OASPL; (e) and (f) RS-25 startup; (g) and (h) SRB ignition; and (i) and (j) 0.5 s period corresponding to maximum OASPL.

pad design results in significant radiation asymmetry during ignition, the vehicle's maximum north-south noise radiation once it lifts off is approximately symmetric. The other noteworthy feature during this maximum OASPL period evident in both Figs. 3(i) and 3(j) are pressure shocks—near instantaneous pressure rises—that result in the far field from nonlinear acoustic propagation and are the cause of the crackling or popping noise associated with rocket launches (Lubert *et al.*, 2022). Given the rapid fluid acceleration, these shocks represent a marked increase in instantaneous acoustic loading.

The final results we show in this letter are maximum one-third octave (OTO) band spectra. Figure 4(a) compares maximum spectra at all five stations from Fig. 2. The spectral calculation interval includes the maximum OASPL segment but is extended over the entire 3 dB-down (re maximum) period. Per Figs. 3(c) and 3(d), this interval can extend 10 s or more (at farther stations). While McInerny (1996) used the 6 dB-down interval in calculating spectra, we have chosen 3 dB because it corresponds to the half-power (full width, half max) interval.

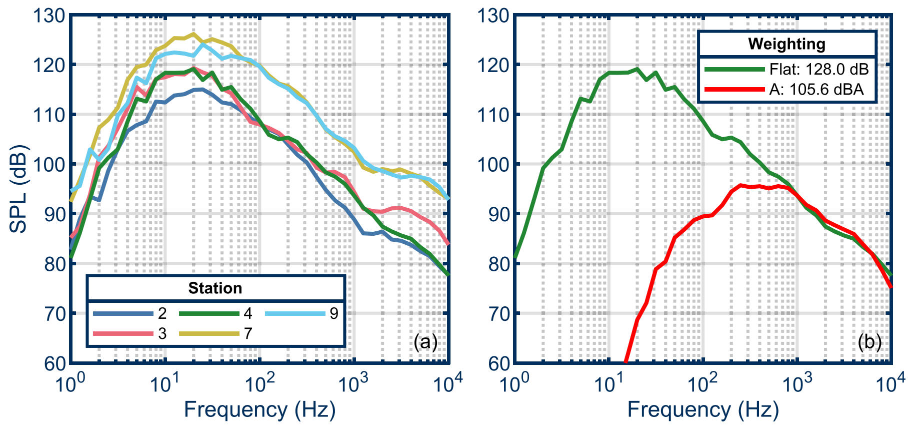

Fig. 4. (a) One-third octave band spectra during the maximum recorded level (3 dB down) time window at each station. (b) A comparison between flat and A-weighted spectra at Station 4, along with their associated overall levels.

The maximum OTO spectra in Fig. 4(a) reveal a similar characteristic shape with a consistent OTO-band peak frequency around 20 Hz and significant high-frequency energy (80–95 dB at 10 kHz) that is associated with the time-domain shocks. However, the spectra also have different relative low- and high-frequency behavior. For example, Stations 7 and 9 have nearly identical high-frequency levels above 100 Hz, despite Station 9 being farther away and having lesser low-frequency levels. Conversely, Stations 3 and 4 share a similar low-frequency spectrum below 1 kHz, but the levels at 10 kHz differ by about 10 dB. Some, but not all, of that difference is likely Station 4's GRAS 47AC high-frequency response (GRAS, 2022) for non-normal incidence of the sound field above 10 kHz; spectral corrections will be pursued once vehicle trajectory data are available. Regarding microphone response, the actual low-frequency response of the 46BE appears markedly better than the 4 Hz cutoff manufacturer specification as there is no noticeable difference in low-frequency slope between Station 4 and any of the other stations. Finally, it is noteworthy that Station 2 has the lowest levels in the vicinity of 20 Hz by more than 3 dB, even though Station 4 is about 1 km farther away (recall that the maximum OASPL at Station 2 was 1.6 dB lower than Station 4). The causes of all these differences need further study, but local weather is one strong possibility. For example, a near-ground meteorological layer of significance is likely, given the broad interference null (spectral dip) that occurs in the ∼1–2 kHz region at some stations. Prior laboratory measurements of the ground plate configuration (Anderson *et al.* 2022) and other rocket measurements [e.g., Mathews *et al.* (2021) and Hart *et al.* (2022)] have not generally revealed these nulls; they appear particular to this launch and measurement environment. Wind direction could be a partial explanation for the lower sound levels at Station 2, as winds at a 40 m height were ∼5 m/s toward north-north-east. These propagation phenomena will be investigated in more detail once trajectory and additional weather data are available.

The levels and spectra thus far have been flat-weighted, but human impacts from noise are often assessed using A-weighted sound levels. One final spectral comparison is that of maximum OTO spectrum and its A-weighted counterpart. Figure 4(b) duplicates Station 4's spectrum from Fig. 4(a) and shows the corresponding A-weighted spectrum, along with flat and A-weighted overall levels. Per the Noise Navigator™ database (Berger *et al.*, 2016), the kinds of A-weighted levels from SLS at Station 4 (5.15 km away) are associated with operating chainsaws (105 dBA) or circular saws (106 dBA) and are a little louder than the average level at a rock concert (104 dBA). Whether these are an accurate subjective impression of an SLS launch should be the subject of future research. However, because shock-containing noise is described in terms of its "crackle" (Gee *et al.*, 2018) and because Noise Navigator™ reports the A-weighted level of crackling Rice Krispies® "fresh in the cereal bowl after milk has just been poured" as 30 dBA, we drily observe that the weighted SLS noise intensity at Station 4 is approximately 40 million times greater than a bowl of audible morning cereal.

In Fig. 4(b), the difference between the flat and A-weighted spectra is striking as the A-weighted spectrum completely misses the rocket's dominant acoustical energy. A-weighting was designed long ago to crudely approximate human hearing at the 40 phon (whisper-like) loudness level and there are few sounds farther from a whisper than a space vehicle launch—both in terms of level and in frequency content. Although we question the use of A-weighted levels as an appropriate measure of characterizing human response to rocket noise, it allows a meaningful comparison to the aforementioned environmental assessments. The 2008 Ares-V modeling (NASA, 2008) extended to SLS (NASA, 2013) predicted the maximum A-weighted level at the Apollo/Saturn-V viewing area [see Fig. 2(a)] would be 98 dBA, and the maximum A-weighted sound level at the VAB would be between 99 and 102 dBA. As shown in Fig. 2(a), Station 4 is near the Saturn-V viewing area and is at a similar distance from LC-39B as the VAB. The SLS maximum A-weighted level at 5.15 km approaches 106 dB, more than 7 dB greater than predicted for the greater-thrust Ares V at the Saturn-V viewing area. Additionally, the Station 4 levels were 4 dB greater than predicted at the VAB. These discrepancies—indicating a greater SLS footprint—suggest the need for further analysis, modeling, and measurements of future Artemis missions.

5. Conclusion

We have briefly described noise measurements associated with liftoff of NASA's Space Launch System's Artemis-I mission at five PUMA stations. Although there are numerous other analyses to pursue, we hope this letter helps communicate the following findings. First, sound waves were of sufficient intensity that the pressure rarefactions formed visible, propagating vapor clouds near the launch pad. Second, the SRB ignition overpressure is a significant transient event that propagates primarily in the direction of the flame trench exit. Third, post-liftoff maximum overall levels at distances of 4–5 km approach 130 dB, nearly 20 dB greater than predicted by environmental assessments. Fourth, SLS one-third-octave band noise spectra at these five stations peak at around 20 Hz, with significant content from below 1 Hz to beyond 10 kHz. The high-frequency energy is associated with shocks that are also responsible for the crackling or popping noise heard during this and other space vehicle launches. Finally, A-weighted measurements, which differ by 4–7 dB from prior environmental assessment predictions, indicate levels at over 5 km from the launchpad that are comparable with chainsaw operation. Future analyses will focus on both source and propagation aspects of Artemis-I launch noise, helping to further characterize the rocket that will take us back to the moon, and beyond.

Acknowledgments

The measurements were supported by the Utah NASA Space Grant Consortium, the BYU College of Physical and Mathematical Sciences, and Rollins College Hugh and Jeannette McKean Faculty Research Grant. We are especially grateful to Chris Parlier of NASA KSC for significant support during measurement planning and implementation. Additionally, we thank John Hueckel, Andrew Swift, and Beatrice Muranaka of NASA Kennedy Space Center, the National Parks Service, John Ellsworth of Brigham Young University, Thomas Moore of Rollins College, Elisha Crean of Harbor Pointe Condominiums, and Charlie and Kathleen Manship for their assistance with different aspects of the measurement campaign.

References and links

Anderson, M. C., Gee, K. L., Novakovich, D. J., Mathews, L. T., and Jones, Z. T. (**2022**). "Comparing two weather robust microphone configurations for outdoor measurements," *Proc. Mtgs. Acoust.* **42**, 040005.

Berger, E. H., Neitzel, R., and Kladden, C. A. (**2016**). "Noise Navigator Sound Level Database," 3M Personal Safety Division, EAR 88-34/HP, available at https://multimedia.3m.com/mws/media/1262312O/3m-noise-navigator.xlsx (Last viewed 23 November 2022).

Eldred, K. M. (**1971**). "Acoustic loads generated by the propulsion system," NASA SP-8072.

Federal Aviation Administration (**2016**). "Adoption of the Environmental Assessment and Finding of No Significant Impact for Multi-Use of Launch Complexes 39A and 39B, John F. Kennedy Space Center, FL," available at https://www.faa.gov/space/environmental/nepa_docs/media/FAA_FONSI_SpaceX_Falcon_Ops-LC_39A-final.pdf (Last viewed 23 November 2022).

Gee, K. L., Mathews, L. T., Anderson, M. C., and Hart, G. W. (**2022**). "Saturn-V sound levels: A letter to the Redditor," J. Acoust. Soc. Am. **152**, 1068–1073.

Gee, K. L., Novakovich, D. J., Mathews, L. T., Anderson, M. C., and Rasband, R. D. (**2020**). "Development of a Weather-Robust Ground-Based System for Sonic Boom Measurements," NASA/CR-2020-5001870, available at https://ntrs.nasa.gov/citations/20205001870 (Last viewed 13 January 2023).

Gee, K. L., Russavage, P. B., Neilsen, T. B., Swift, S. H., and Vaughn, A. B. (**2018**). "Subjective rating of the jet noise crackle percept," J. Acoust. Soc. Am. **144**, EL40–EL45.

GRAS (**2022**). "GRAS 47AC Microphone Specifications," https://www.grasacoustics.com/products/special-microphone/infra-sound-microphones/product/712-47ac (Last viewed 23 November 2022).

Hart, G. W., Mathews, L. T., Anderson, M. C., Durrant, J. T., Bassett, M. S., Olausson, S. A., Houston, G., and Gee, K. L. (**2022**). "Methods and results of acoustical measurements made of a Delta IV Heavy launch," Proc. Mtgs. Acoust. **45**, 040003.

Ikawa, H., and Laspesa, F. S. (**1985**). "Ignition/duct overpressure induced by Space Shuttle solid rocket motor ignition," J. Spacecr. Rockets **22**, 481–488.

James, M., Salton, A., Calton, M., Downing, M., Gee, K. L., and McInerny, S. A. (**2020a**). "Commercial space operations noise and sonic boom measurements," Contractor's Final Rep. ACRP Project 02-81, available at https://www.trb.org/ACRP/Blurbs/180769.aspx (Last viewed 13 January 2023).

James, M. M., Salton, A. R., Calton, M. F., and Lympany, S. V. (**2020b**). "RUMBLE Version 3.0 User Guide," Blue Ridge Research and Consulting, LLC, Asheville, North Carolina, https://onlinepubs.trb.org/onlinepubs/acrp/acrp_wod_051RumbleGuide.pdf (Last viewed 22 November 2022).

Lubert, C. P., Gee, K. L., and Tsutsumi, S. (**2022**). "Supersonic jet noise from launch vehicles: 50 years since NASA SP-8072," J. Acoust. Soc. Am. **151**, 752–791.

Margasahayam, R., and Caimi, R. (**1999**). "Rocket noise prediction program," NASA Technical Reports Server, Doc. No. 19990040528.

Mathews, L. T., Gee, K. L., and Hart, G. W. (**2021**). "Characterization of Falcon 9 launch vehicle noise from far-field measurements," J. Acoust. Soc. Am. **150**, 620–633.

McInerny, S. A. (**1992**). "Characteristics and predictions of far-field rocket noise," Noise Control Eng. J. **38**(1), 5–16.

McInerny, S. A. (**1996**). "Launch vehicle acoustics Part 1: Overall levels and spectral characteristics," J. Aircraft **33**, 511–517.

Nance, D. K., and Liever, P. A. (**2015**). "Space launch system scale model acoustic test ignition overpressure testing," in *Aerospace Testing Conference M15-4899*, Los Angeles, CA, https://ntrs.nasa.gov/citations/20150021452 (Last viewed 23 November 2022).
NASA (**2008**). "Final Constellation Programmatic Environmental Impact Statement," John F. Kennedy Space Center, Florida, January 2008, https://www.nasa.gov/pdf/207916main_Cx_PEIS_final_Executive_Summary.pdf (Last viewed 23 November 2022).
NASA (**2013**). "Final Environmental Assessment for Multi-Use of Launch Complexes 39A and 39B," John F. Kennedy Space Center, Florida, November 2013, https://netspublic.grc.nasa.gov/main/finalMultiuseEA.pdf (Last viewed 23 November 2022).
NASA (**2022**). https://images-assets.nasa.gov/video/KSC-20221116-MH-AJN01-0001-Artemis_I_Isolated_Launch_Views-3314595/KSC-20221116-MH-AJN01-0001-Artemis_I_Isolated_Launch_Views-3314595~orig.mp4 (Last viewed 23 November 2022).